

rather than decrease as is observed.

A  $T_1$ - $T_1$  annihilation mechanism also provides a basis for describing the two distributions in the  $T_1$  carotenoid population. For  $T_1$ - $T_1$  annihilation to be an effective  $T_1$  decay route, the  $T_1$  molecules must be at or near van der Waals distances to each other. This distance restriction would seem to prohibit  $T_1$ - $T_1$  annihilation with a  $T_1$  carotenoid concentration of only 1  $\mu$ M or 1% of the total carotenoid population. However, it must be emphasized that the  $T_1$  carotenoids are formed by singlet fission as adjacent triplet pairs, at van der Waals distances, and annihilation should simply be considered as the reverse reaction. Triplet formation would then be described with a  $<6$  ps time constant and  $T_1$ - $T_1$  annihilation described by an approximately 80-ps time constant. Competitive with  $T_1$ - $T_1$  annihilation is rapid triplet energy transfer (i.e., triplet diffusion) that results in the

separation of the triplet pairs from each other. These remaining  $T_1$  carotenoids are then located far enough from one another to prevent  $T_1$ - $T_1$  annihilation and, consequently, relax via the slower, normal intersystem crossing mechanism. This interpretative model remains speculative, and further experimentation is required to more completely characterize the phenomenon.

**Acknowledgment.** The authors gratefully acknowledge the technical assistance of T. L. Brack. Partial support for this work was provided by a grant from the DuPont Corporation for the exchange of Japanese and American researchers. G.H.A. thanks the Alexander von Humboldt-Stiftung and Professor E. Schlag for their support and hospitality at the Technical University of Munich where part of this manuscript was prepared.

Registry No. Rhodopin, 105-92-0; spirilloxanthin, 34255-08-8.

## $^{89}\text{Y}$ MAS NMR Study of Rare-Earth Pyrochlores: Paramagnetic Shifts in the Solid State

Clare P. Grey,<sup>†</sup> Mark E. Smith,<sup>‡</sup> Anthony K. Cheetham,<sup>\*,†</sup> Christopher M. Dobson,<sup>§</sup> and Ray Dupree<sup>‡</sup>

Contribution from the Chemical Crystallography Laboratory, University of Oxford, 9 Parks Road, Oxford OX1 3PD, U.K., Inorganic Chemistry Laboratory, University of Oxford, South Parks Road, Oxford OX1 3QR, U.K., and Physics Department, University of Warwick, Coventry CV4 7AL, U.K. Received June 9, 1989

**Abstract:**  $^{89}\text{Y}$  MAS NMR spectra have been obtained from yttrium pyrochlores  $\text{Y}_{2-x}\text{Ln}_x\text{M}_2\text{O}_7$  (Ln = Ce, Pr, Nd, Sm, Eu, Yb; M = Sn, Ti). Incorporation of the paramagnetic ions into the diamagnetic compounds was found to cause large reductions in the  $^{89}\text{Y}$  nuclear relaxation times enabling spectra to be accumulated in relatively short times in comparison to similar diamagnetic systems. In addition to the resonances of the diamagnetic end-member compounds,  $\text{Y}_2\text{Sn}_2\text{O}_7$  and  $\text{Y}_2\text{Ti}_2\text{O}_7$ , extra  $^{89}\text{Y}$  resonances were observed, due to the substitution of paramagnetic ions into the local coordination sphere surrounding an  $^{89}\text{Y}$  nucleus. The paramagnetic shifts were found to be proportional to the number of lanthanide ions substituted for yttrium in the first coordination sphere; the intensities of the resonances could be used to determine the concentration of paramagnetic rare-earth ions in the diamagnetic phase. The direction and magnitude of the shifts induced by the presence of paramagnetic ions suggest that there could be a significant contribution from a dipolar mechanism.

High-resolution solid-state NMR, using a wide variety of different nuclei, has proved to be of considerable value in studies of a wide range of both crystalline and amorphous inorganic materials. The many diverse applications have included the elucidation of structure, dynamics, and reaction mechanisms.<sup>1</sup> However, for many nuclei, despite their chemical importance, lack of resolution, low sensitivity, and long relaxation times can restrict the systems that can be studied and limit the information that can be obtained. One approach to assist in the study of such materials is to exploit some of the effects of incorporating paramagnetic ions into solids. The use of low concentrations of iron and manganese to reduce the relaxation times of  $^{29}\text{Si}$  nuclei in glasses and cements is already established,<sup>2,3</sup> as is the use of copper to reduce the recycle delays in the magic angle spinning (MAS) NMR of biomolecules.<sup>4</sup> In general, however, paramagnetic ions have, as yet, been little exploited in the solid state, despite their widespread use as shift and relaxation probes in solution.<sup>5-7</sup> Paramagnetic lanthanides are particularly suitable for study since they all, except  $\text{Gd}^{3+}$ , have short electron relaxation times<sup>6-8</sup> and hence may not always cause excessive broadening of resonances in the NMR spectra. Indeed, it has recently become apparent that it is possible to both obtain and interpret high-resolution NMR spectra from solids containing paramagnetic lanthanides. In

addition to  $^{13}\text{C}$  MAS NMR studies of lanthanide acetates,<sup>9,10</sup> which are molecular structures, the applicability of MAS NMR to the study of paramagnetic continuous solids has been demonstrated,<sup>11,12</sup> particularly in probing local order in solid solutions. The latter studies, which used  $^{119}\text{Sn}$ , yielded a dramatic increase

- (1) Fyfe, C. A. *Solid State NMR for Chemists*; C.F.C. Press: Guelph, Ontario, Canada, 1983; pp 6-7.
- (2) Fujita, T.; Ogino, M. *J. Non-Cryst. Solids* **1984**, *64*, 287-290. Dupree, R.; Holland, D.; McMillan, P. W.; Petifer, R. F. *J. Non-Cryst. Solids* **1984**, *68*, 399-410.
- (3) Dobson, C. M.; Gøberdhan, D. G. C.; Ramsey, J. D. F.; Rodger, S. A. *J. Mater. Sci.* **1988**, *23*, 4108-4114.
- (4) Ganapathy, S.; Naito, A.; McDowell, C. A. *J. Am. Chem. Soc.* **1981**, *103*, 6011-6015.
- (5) Hinckley, C. C. *J. Am. Chem. Soc.* **1969**, *91*, 5160-5162.
- (6) Dobson, C. M.; Levine, B. A. *New Techniques in Biophysics and Cell Biology*; Pain, R. H., Smith, B. J., Eds.; Wiley-Interscience: New York, 1976; Vol. 3, pp 19-90.
- (7) Inagaki, F.; Miyazawa, T. *Progress in NMR Spectroscopy*; Pergamon Press: New York, 1981; Vol. 14, pp 67-111.
- (8) Alsaadi, B. M.; Rossotti, F. J. C.; Williams, R. J. P. *J. Chem. Soc., Dalton Trans.* **1980**, 2147-2150.
- (9) Chacko, V. P.; Ganapathy, S.; Bryant, R. G. *J. Am. Chem. Soc.* **1983**, *105*, 5491-5492. Ganapathy, S.; Chacko, V. P.; Bryant, R. G.; Etter, M. C. *J. Am. Chem. Soc.* **1986**, *108*, 3159-3165.
- (10) Campell, G. C.; Crosby, R. C.; Haw, J. F. *J. Magn. Reson.* **1986**, *69*, 191-195.
- (11) Cheetham, A. K.; Dobson, C. M.; Grey, C. P.; Jakeman, R. J. B. *Nature (London)* **1987**, *328*, 706-707.
- (12) Grey, C. P.; Dobson, C. M.; Cheetham, A. K.; Jakeman, R. J. B. *J. Am. Chem. Soc.* **1989**, *111*, 505-511.

<sup>†</sup> Chemical Crystallography Laboratory, University of Oxford.

<sup>‡</sup> University of Warwick.

<sup>§</sup> Inorganic Chemistry Laboratory, University of Oxford.

in the resolution of the different local environments and a decrease in nuclear  $T_1$  relaxation times, compared with similar diamagnetic systems. Copper(II) compounds have also been studied,<sup>13,14</sup> and the  $^1\text{H}$  MAS NMR spinning sidebands of copper(II) chloride dihydrate have been interpreted in detail.<sup>15</sup>

This paper is concerned with the study, using  $^{89}\text{Y}$  NMR, of rare-earth-doped yttrium stannates and titanates ( $\text{Y}_2\text{Sn}_2\text{O}_7$  and  $\text{Y}_2\text{Ti}_2\text{O}_7$ ), and both extends and complements the previous  $^{119}\text{Sn}$  work<sup>11,12</sup> on lanthanide tin pyrochlores. These compounds have recently been shown to be very effective catalysts for the oxidative coupling of methane.<sup>16</sup> The problems involved in obtaining  $^{89}\text{Y}$  NMR spectra, which result from the very long relaxation times of this nucleus and poor sensitivity due to its low  $\gamma$ , are severe,<sup>17</sup> but the incorporation of paramagnetic ions into the systems studied has proved to be extremely valuable. The compounds all adopt the pyrochlore structure, with only one positional parameter,  $x$ , which determines the position of one of the independent oxygen atoms.<sup>18a</sup> As  $x$  varies between 0.3125<sup>18b</sup> and 0.375, the coordination at the yttrium site becomes progressively less axially distorted; when  $x = 0.375$ , the oxygen coordination around an yttrium forms a perfect cube. The  $x$  parameters for  $\text{Y}_2\text{Sn}_2\text{O}_7$  and  $\text{Y}_2\text{Ti}_2\text{O}_7$  are 0.338<sup>19</sup> and 0.327,<sup>20</sup> respectively; thus, the yttrium site in the titanate is more distorted from cubic symmetry than the site in the stannate. Rare-earth cations can be doped into the yttrium site in these compounds, the degree of substitution depending on the similarity in ionic radii of the  $\text{Y}^{3+}$  and the dopant ion. Although the pyrochlores  $\text{Ce}_2\text{Sn}_2\text{O}_7$  and  $\text{Ce}_2\text{Ti}_2\text{O}_7$  have not been synthesized,<sup>18</sup> the substitution of  $\text{Ce}^{3+}$  into the yttrium pyrochlores was achieved in this study.

### Experimental Section

Polycrystalline samples of the pyrochlores were prepared from stoichiometric quantities of calcined rare-earth oxides and tin(IV) or titanium(IV) oxides. These were ground together and fired in air at 1350 °C for 3–4 days. The cerium-doped samples were prepared slightly differently, using  $\text{Ce}(\text{NO}_3)_3 \cdot 6\text{H}_2\text{O}$  and firing in a  $\text{N}_2$  atmosphere in order to inhibit oxidation of  $\text{Ce}^{3+}$  to  $\text{Ce}^{4+}$ . All the samples were characterized by X-ray powder diffraction.

The MAS NMR spectra were collected on a Bruker MSL-360 spectrometer operating at 17.646 MHz for  $^{89}\text{Y}$ . Magic angle spinning was carried out with 7-mm double-bearing alumina rotors at spinning speeds of approximately 3500 Hz. Long recycle times of typically 45 s, combined with  $\pi/6$  pulses, were used to obtain  $^{89}\text{Y}$  spectra from the diamagnetic pyrochlores; spectra with good signal to noise ratios required approximately 200 scans. Spectra from the paramagnetic pyrochlores were accumulated by using much shorter recycle times of 1–2 s, but required a larger number of scans (900–2400) than used for the diamagnetic compounds. Preacquisition delays of 100  $\mu\text{s}$ , to eliminate probe ring down, were used when acquiring all the spectra. Variable-temperature NMR measurements were carried out by altering the temperature of the bearing gas and allowing the temperature to equilibrate before accumulating the spectra. The temperature of the bearing gas was monitored as it left the stator block. Errors bars have been included in the experimental results to account for any differences between the measured temperature and the actual temperature of the sample. Chemical shifts were referenced by using 1 M aqueous  $\text{YCl}_3$  as an external standard. The spectra were processed with line broadening of typically 25 and 70 Hz for the diamagnetic and paramagnetic compounds, respectively.

### Results and Discussion

**1.  $^{89}\text{Y}$  Spectra of the Yttrium Pyrochlores.** The  $^{89}\text{Y}$  MAS NMR spectra of  $\text{Y}_2\text{Sn}_2\text{O}_7$  and  $\text{Y}_2\text{Ti}_2\text{O}_7$  are presented in Figure

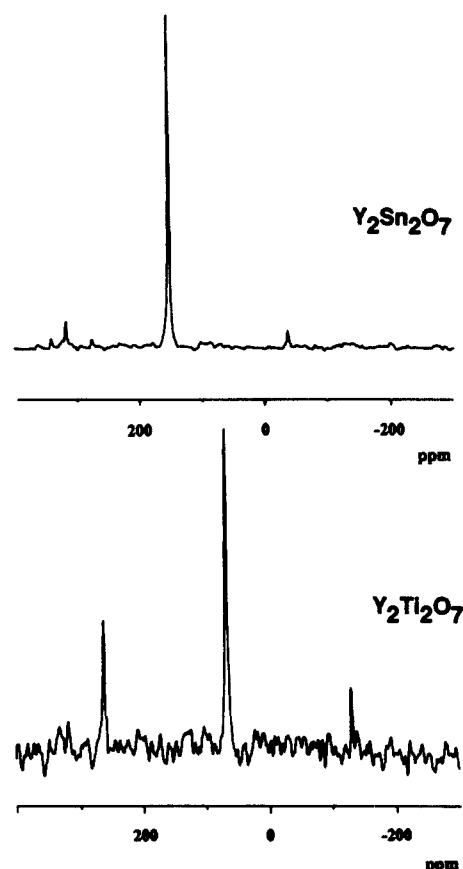


Figure 1.  $^{89}\text{Y}$  MAS NMR of the pyrochlores  $\text{Y}_2\text{Sn}_2\text{O}_7$  and  $\text{Y}_2\text{Ti}_2\text{O}_7$  collected by using a recycle time of 45 s. Chemical shifts are quoted relative to 1 M aqueous  $\text{YCl}_3$ .

1; both samples give only one resonance, at +150 ppm for  $\text{Y}_2\text{Sn}_2\text{O}_7$  and +65 ppm for  $\text{Y}_2\text{Ti}_2\text{O}_7$ , consistent with there being only one crystallographically distinct yttrium site in each compound.<sup>18</sup> Even at fast spinning speeds, the greater chemical shift anisotropy at the yttrium site in  $\text{Y}_2\text{Ti}_2\text{O}_7$  is apparent from the intensities of the spinning sidebands. Analysis of the sideband patterns<sup>21</sup> at slower speeds gives values for the chemical shift tensors of  $240 \pm 20$ ,  $210 \pm 15$ , and  $0 \pm 10$  ( $\delta_1$ ,  $\delta_2$ , and  $\delta_3$ ) for  $\text{Y}_2\text{Sn}_2\text{O}_7$  and  $275 \pm 30$ ,  $260 \pm 20$ , and  $-340 \pm 50$  for  $\text{Y}_2\text{Ti}_2\text{O}_7$ . These chemical shift anisotropies are the largest so far reported in the  $^{89}\text{Y}$  NMR of diamagnetic yttrates,<sup>17,22</sup> consistent with the large axial distortions of the oxygen coordination polyhedra reported in these compounds, the distortion being larger for the yttrium titanate than for the stannate.

The  $^{89}\text{Y}$  spectra of the samples  $\text{Y}_{1.7}\text{Nd}_{0.3}\text{Sn}_2\text{O}_7$  and  $\text{Y}_{1.7}\text{Eu}_{0.3}\text{Sn}_2\text{O}_7$ , collected by using short recycle times of 2 s, are presented in Figure 2; two resonances are observed in the spectrum of the former and three in the spectrum of the latter. The resonance at +150 ppm, present in both spectra, is broader than the resonance from  $\text{Y}_2\text{Sn}_2\text{O}_7$  but at the same chemical shift (the widths at half-height for this resonance are 110 Hz in  $\text{Y}_2\text{Sn}_2\text{O}_7$  and 220 Hz in  $\text{Y}_{1.7}\text{Nd}_{0.3}\text{Sn}_2\text{O}_7$ ). The new peaks are downfield at +188 ppm in the  $\text{Y}_{1.7}\text{Nd}_{0.3}\text{Sn}_2\text{O}_7$  spectrum and upfield at +71 and -8 ppm in the  $\text{Y}_{1.7}\text{Eu}_{0.3}\text{Sn}_2\text{O}_7$  spectrum. When the spectra were acquired by using longer recycle times, the intensity of the resonance at +150 ppm was seen to increase relative to the new resonances in both cases. In these and the subsequent spectra, the resonances occurring at the same chemical shift as the original diamagnetic end-member compounds are labeled A; any new resonances are labeled B–D, in order of chemical shift difference from A. This is in line with the notation used previously.<sup>11,12</sup>  $^{89}\text{Y}$  spectra were collected from further samples of  $\text{Y}_{1.7}\text{Ln}_{0.3}\text{Sn}_2\text{O}_7$ ,

(21) Herzfeld, J.; Berger, A. E. *J. Chem. Phys.* 1980, 73, 6021–6030.

(22) Thompson, A. R.; Oldfield, E. *J. Chem. Soc., Chem. Commun.* 1987, 647–648.

(13) Hall, L. D.; Lim, T. K. *Carbohydr. Res.* 1986, 148, 13–20.

(14) Walter, T. H.; Oldfield, E. *J. Chem. Soc., Chem. Commun.* 1987, 647–648.

(15) Nayeem, A.; Yesinowski, J. P. *J. Chem. Phys.* 1988, 89, 4600–4608.

(16) Ashcroft, A.; Cheetham, A. K.; Green, M. L. H.; Grey, C. P.; Vernon, P. D. *J. Chem. Soc., Chem. Commun.* 1989, 1667–1669.

(17) Dupree, R.; Smith, M. E. *Chem. Phys. Lett.* 1988, 148, 41–44.

(18) (a) Subramanian, M. A.; Aravamudan, G.; Subba Rao, G. V. *Prog. Solid State Chem.* 1980, 15, 55–143. (b) There are four choices of origin for a cubic pyrochlore and the values of the  $x$  parameter will be different for each. Those quoted here, are for an origin at the B atom (i.e., Sn or Ti).

(19) Brisse, F.; Knop, O. *Can. J. Chem.* 1968, 46, 859.

(20) Knop, O.; Brisse, F.; Castelli, L. *Can. J. Chem.* 1969, 47, 971.

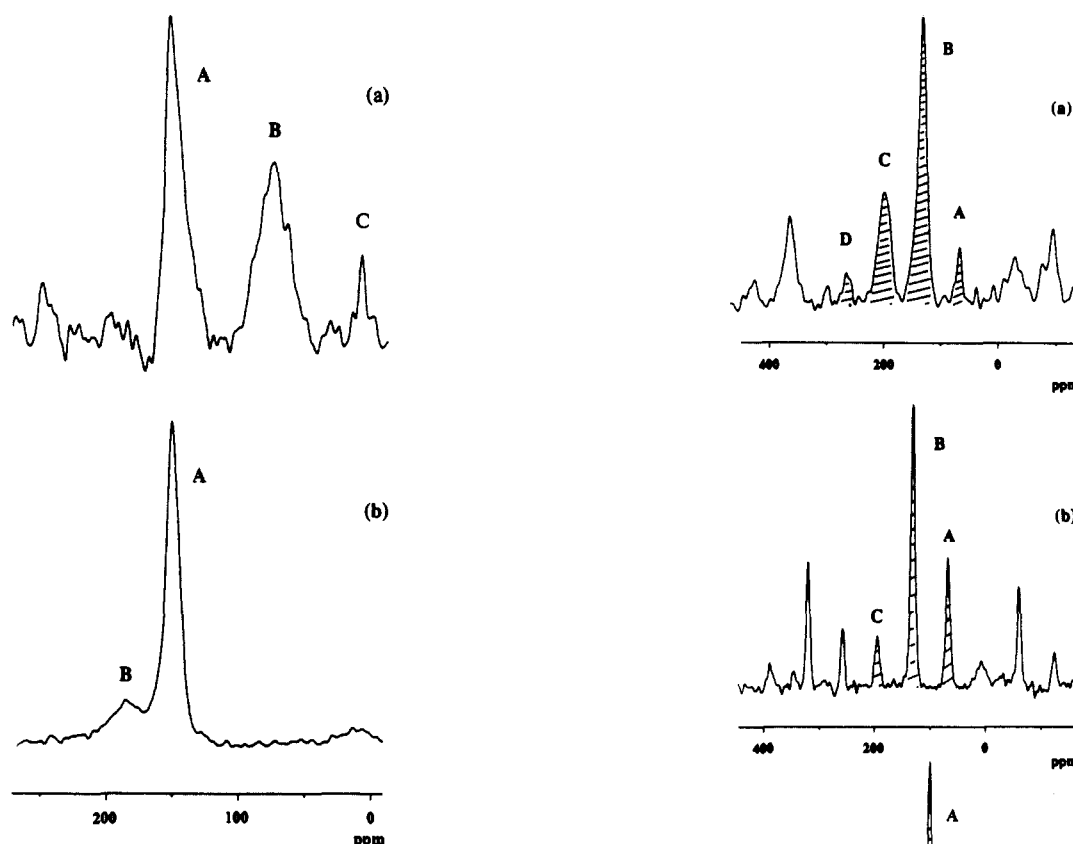


**Figure 2.**  $^{89}\text{Y}$  MAS NMR of the samples of composition  $\text{Y}_{1.7}\text{Eu}_{0.3}\text{Sn}_2\text{O}_7$  (a) and  $\text{Y}_{1.7}\text{Nd}_{0.3}\text{Sn}_2\text{O}_7$  (b) collected with recycle times of 2 s. The isotropic resonances are labeled A–C (see text); all the other peaks are spinning sidebands.

**Table I.** Difference in Isotropic Chemical Shift between the Two Resonances Labeled A and B in the  $^{89}\text{Y}$  MAS NMR of the Rare-Earth-Doped Yttrium Pyrochlores Compared with the  $^{119}\text{Sn}$  Chemical Shifts of the Lanthanide Stannates from ref 12 (at Room Temperature)

ion	$^{89}\text{Y}$ shift diff, ppm		$^{119}\text{Sn}$ chem shift of $\text{Ln}_2\text{Sn}_2\text{O}_7$ , <sup>a</sup> ppm
	$\text{Y}_{2-x}\text{Ln}_x\text{Sn}_2\text{O}_7$	$\text{Y}_{2-x}\text{Ln}_x\text{Ti}_2\text{O}_7$	
$\text{Y}^{3+}$	0	0	0
$\text{Ce}^{3+}$	21	24	<sup>c</sup>
$\text{Pr}^{3+}$	82	65	$-3670 \pm 50$
$\text{Nd}^{3+}$	38	65	$-3580 \pm 50$
$\text{Sm}^{3+}$	<sup>b</sup>	5	$+490$
$\text{Eu}^{3+}$	-79	-104	$+5480 \pm 200$
$\text{Ho}^{3+}$	<sup>b</sup>	<sup>b</sup>	<sup>d</sup>
$\text{Tm}^{3+}$	<sup>b</sup>	<sup>b</sup>	$+1780 \pm 400$
$\text{Yb}^{3+}$	-60	-66	$-10 \pm 50$

<sup>a</sup>Relative to the  $^{119}\text{Sn}$  chemical shift of  $\text{Y}_2\text{Sn}_2\text{O}_7$ . <sup>b</sup>Only resonance A was obtained. <sup>c</sup> $\text{Ce}_2\text{Sn}_2\text{O}_7$  does not exist. <sup>d</sup>No  $^{119}\text{Sn}$  resonance was detected for  $\text{Ho}_2\text{Sn}_2\text{O}_7$ .

$\text{Ln} = \text{Ce}, \text{Pr}, \text{Sm}, \text{Ho}, \text{Tm}, \text{and Yb}$ . Two peaks were again visible in the spectra for  $\text{Ln} = \text{Ce}, \text{Pr}, \text{and Yb}$ , the peak B occurring at +172, +232, and +90 ppm, respectively, and the peak A remaining at +150 ppm in all cases. No resonances, other than the one at +150 ppm (peak A), were visible in the spectra from the  $\text{Y}_{1.7}\text{Sm}_{0.3}\text{Sn}_2\text{O}_7$ ,  $\text{Y}_{1.7}\text{Ho}_{0.3}\text{Sn}_2\text{O}_7$ , and  $\text{Y}_{1.7}\text{Tm}_{0.3}\text{Sn}_2\text{O}_7$  samples.

Spectra from the titanium pyrochlore solid solutions,  $\text{Y}_{1.9}\text{Pr}_{0.1}\text{Ti}_2\text{O}_7$  and  $\text{Y}_{1.7}\text{Nd}_{0.3}\text{Ti}_2\text{O}_7$ , collected with a recycle time of 1 s, are presented in Figure 3a and b. Three resonances are visible in the spectrum of the former (labeled A–C) and four resonances (labeled A–D) can be seen in the spectrum of the latter. The shift differences between peaks A and B, B and C, and C and D are equal for each individual solid solution. Figure 3c shows the spectrum of the  $\text{Y}_{1.9}\text{Pr}_{0.1}\text{Ti}_2\text{O}_7$  sample collected by use of a longer recycle time. The intensity of peak A is seen to increase

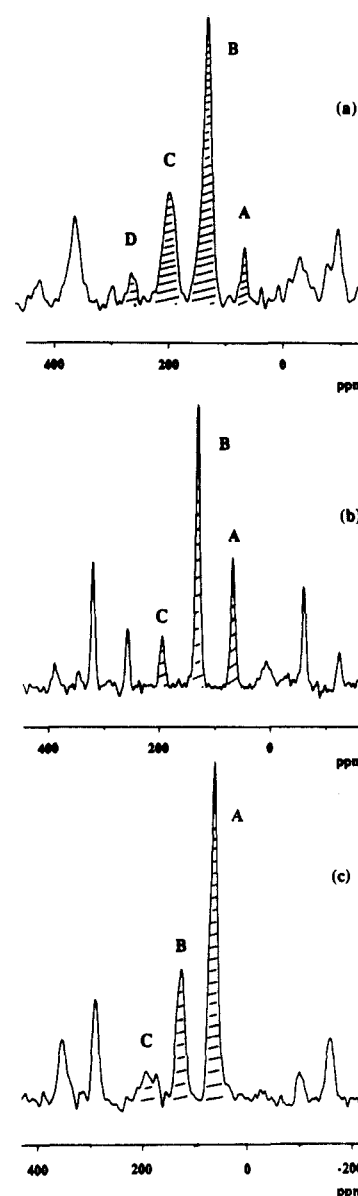


**Figure 3.**  $^{89}\text{Y}$  MAS NMR of the samples of composition  $\text{Y}_{1.7}\text{Nd}_{0.3}\text{Ti}_2\text{O}_7$  (a) and  $\text{Y}_{1.9}\text{Pr}_{0.1}\text{Ti}_2\text{O}_7$  (b) collected with recycle times of 1 s. The spectrum from the latter sample was also collected by using a longer recycle time of 45 s (c). Greater line broadening has been applied when processing this spectrum due to the poorer signal to noise ratio obtained, compared with spectra in a and b. The isotropic resonances are labeled and shaded; all the other peaks are spinning sidebands.

relative to peaks B and C as the recycle time is increased, implying that peaks B–D have much shorter spin–lattice ( $T_1$ ) relaxation times than peak A. Three resonances A–C, are observed in spectra collected by using short recycle times from  $\text{Y}_{1.9}\text{Yb}_{0.1}\text{Ti}_2\text{O}_7$  (not shown here) and  $\text{Y}_{1.9}\text{Eu}_{0.1}\text{Ti}_2\text{O}_7$ , while only two resonances are observed in the spectra from  $\text{Y}_{1.9}\text{Sm}_{0.1}\text{Ti}_2\text{O}_7$  and  $\text{Y}_{1.9}\text{Ce}_{0.1}\text{Ti}_2\text{O}_7$  samples. Figure 4 shows the spectrum of  $\text{Y}_{1.9}\text{Eu}_{0.1}\text{Ti}_2\text{O}_7$  collected with a long recycle time; the third resonance C is now not visible above the noise. The values of the differences in chemical shift between peak A and peak B for all the samples are collated in Table I, and it should be noted that the shifts observed in the spectra of the titanates, for a particular lanthanide dopant, are generally larger than for those for the stannates. No resonances, apart from A, were visible for spectra collected from samples of  $\text{Y}_{2-y}\text{Ho}_y\text{Ti}_2\text{O}_7$  and  $\text{Y}_{2-y}\text{Tm}_y\text{Ti}_2\text{O}_7$ , despite use of a variety of different dopant concentrations (from  $y = 0.01$ –0.2).

The above spectra can be rationalized in a similar way to the  $^{119}\text{Sn}$  spectra obtained from the solid solutions of  $\text{Y}_{2-y}\text{Sm}_y\text{Sn}_2\text{O}_7$ <sup>11,12</sup> and result from substitution of a paramagnetic ion for yttrium in the local coordination surrounding the central  $^{89}\text{Y}$  nucleus. This

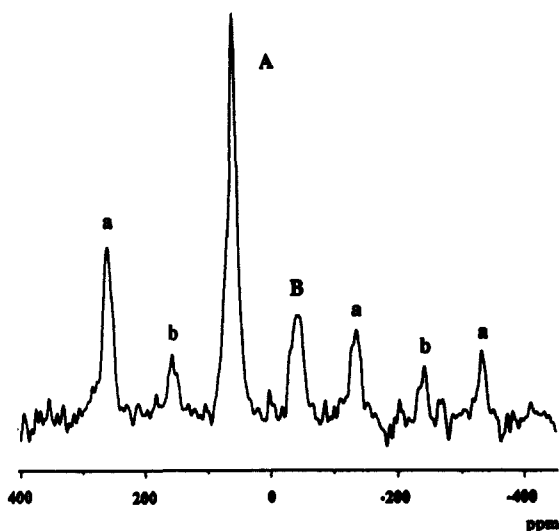


Figure 4. Spectrum from a sample of composition  $Y_{1.9}Eu_{0.1}Ti_2O_7$  collected with a recycle time of 60 s. A and B are the isotropic resonances; a and b are their spinning sidebands.

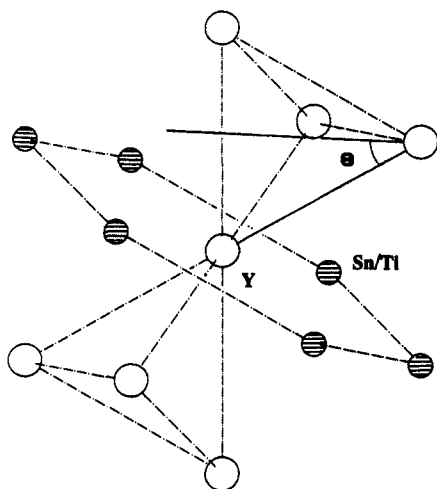


Figure 5. Coordination around an yttrium atom in  $Y_2M_2O_7$  ( $M = Sn, Ti$ ).  $\theta$  is the angle between the  $C_3$  symmetry axis at the Y site and the internuclear axis joining this site with a next nearest Y atom.

causes both a shift in the <sup>89</sup>Y resonance from the chemical shift of the diamagnetic end member and a decrease in the spin-lattice relaxation time ( $T_1$ ). Referring to Figure 5, an yttrium atom is seen to be coordinated to six equivalent yttriums through Y–O–Y bonds in the diamagnetic end member. Hence, peak B results from the yttrium local environment  $Y(OY)_5(OLn)$ , where Ln is a paramagnetic ion, peak C from  $Y(OY)_4(OLn)_2$ , etc. Since peaks A–D are equally spaced, the <sup>89</sup>Y shift on substituting a paramagnetic ion into the local coordination of an yttrium atom is additive. Resonances resulting from <sup>89</sup>Y environments  $Y(OY)_{6-x}(OLn)_x$ , where  $x > 3$  were not observed, presumably due to the limited concentrations of paramagnetic ions doped into the  $Y_2M_2O_7$  phase.

The above interpretation of the shifts suggests that the compositions of solid solutions can be obtained from their <sup>89</sup>Y spectra; this was explored in detail in this work for two samples. It proved possible to calculate the actual composition of the sample of notional stoichiometry  $Y_{1.9}Eu_{0.1}Ti_2O_7$ , by using the relative intensities of the resonances A–C. The ratio of resonances A and B was obtained from a spectrum collected by using a long recycle time (Figure 4), while the ratio of resonances B and C was obtained from a spectrum collected with a recycle delay of 4 s, in which only peak A was saturated. Relative intensities of 73.3:23.2:3.43 for A:B:C, including intensities of their respective spinning sidebands, were obtained and these gave a composition of  $Y_{1.90}Eu_{0.10}Ti_2O_7$ . As this corresponds to the bulk composition

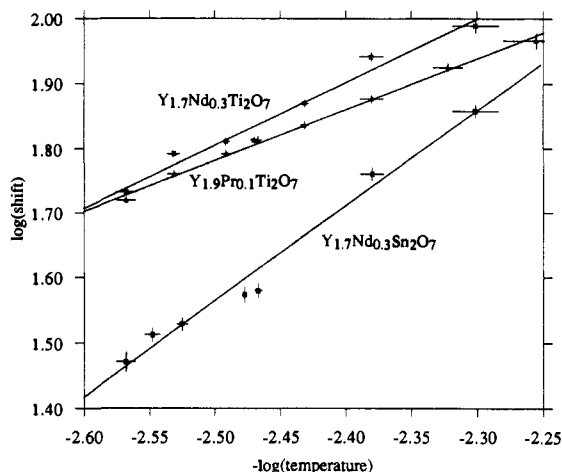


Figure 6. Temperature dependences of the shifts caused by the paramagnetic ions, in the three samples  $Y_{1.7}Nd_{0.3}Sn_2O_7$ ,  $Y_{1.7}Nd_{0.3}Ti_2O_7$ , and  $Y_{1.9}Pr_{0.1}Ti_2O_7$ . The isotropic chemical shift of resonance A was found to vary slightly with temperature, hence the log of the shift from resonance A to B is plotted against  $-\log$  temperature (in Kelvin)].

of the sample, a solid solution of  $Eu_2Ti_2O_7$  in  $Y_2Ti_2O_7$  is present for  $y = 0.1$ . The calculation was repeated for the sample of composition  $Y_{1.7}Eu_{0.3}Sn_2O_7$ . Intensities of 67.4:28.2:4.43 for A:B:C, obtained by a similar method as employed above, indicated a solid solution limit of composition  $Y_{1.88}Eu_{0.12}Sn_2O_7$ . It was clear from the X-ray powder pattern that the remaining  $Eu^{3+}$  was present in the form of  $Eu_2Sn_2O_7$  and a very small amount of  $Eu_2O_3$ .

The difference in chemical shift between resonances A and B, which was investigated in three of the samples, increased substantially with reduction in temperature. The shifts observed in the sample  $Y_{1.7}Nd_{0.3}Sn_2O_7$  have a temperature dependence of approximately  $T^{-1.5}$  in the temperature range 200–370 K (Figure 6). However, the shifts in the samples  $Y_{1.7}Nd_{0.3}Ti_2O_7$  and  $Y_{1.9}Pr_{0.1}Ti_2O_7$  are closer to a  $T^{-1}$  dependence over a similar range of temperatures (approximately  $T^{-1.0}$  and  $T^{-0.8}$ , respectively).

**2. Origin of the Shifts.** The shifts in the <sup>89</sup>Y MAS NMR spectra produced on substituting a paramagnetic lanthanide ion into the first coordination sphere around an yttrium atom can be compared with the shifts obtained in the <sup>119</sup>Sn MAS NMR spectra of the paramagnetic stannates,  $Ln_2Sn_2O_7$ , (Table I). The <sup>89</sup>Y shifts are approximately an order of magnitude smaller for each lanthanide than those of <sup>119</sup>Sn. Furthermore, the shifts in the <sup>89</sup>Y and <sup>119</sup>Sn spectra, except those from the ytterbium and samarium samples, are in opposite directions.

There are two dominant shift mechanisms, apart from the "normal" isotropic chemical shift, that contribute to the isotropic chemical shift of a paramagnetic compound.<sup>6,7</sup> Delocalization of unpaired electron spin density gives rise to a through bond or Fermi contact shift, while anisotropy in the magnetic susceptibility of the paramagnetic ion can result in a through space, dipolar (or "pseudocontact") shift. That the observed shifts are additive depending on the number of next nearest neighbors is consistent with both mechanisms, since an yttrium atom is surrounded by six equivalent yttrium atoms.

The change in the effective magnetic field  $\Delta H$  at the NMR nucleus due to the Fermi interaction with the unpaired f electrons is<sup>23</sup>

$$\Delta H = a_n \langle S_z \rangle / \gamma h$$

where  $\gamma$  is the gyromagnetic ratio (negative for both <sup>119</sup>Sn and <sup>89</sup>Y nuclei),  $a_n$  the electron–nucleus hyperfine coupling constant, and  $\langle S_z \rangle$  the expectation value of the z component of the rare-earth spin. Values for  $\langle S_z \rangle$  have been calculated for the  $Ln^{3+}$  ions by Golding and Halton.<sup>24a</sup> The <sup>119</sup>Sn NMR shifts have already been

(23) Carrington, A.; McLachlan, A. D. *Introduction to Magnetic Resonance*; Harper and Row, Inc.: New York, 1967; p 222.

**Table II.** Relative Pseudocontact Shifts for Different Lanthanides,<sup>a</sup> Together with Crystal Field Parameters Obtained from Mössbauer Data<sup>b</sup>

ion	rel pseudocontact shift	$A_2^0\langle r^2 \rangle$ , cm <sup>-1</sup>		predicted pseudocontact shift, ppm	
		Ln <sub>2</sub> Sn <sub>2</sub> O <sub>7</sub>	Ln <sub>2</sub> Ti <sub>2</sub> O <sub>7</sub>	Y <sub>2-x</sub> Ln <sub>x</sub> Sn <sub>2</sub> O <sub>7</sub>	Y <sub>2-x</sub> Ln <sub>x</sub> Ti <sub>2</sub> O <sub>7</sub>
Y <sup>3+</sup>	0			0	0
Ce <sup>3+</sup>	-6			71	130
Pr <sup>3+</sup>	-11			130	230
Nd <sup>3+</sup>	-4.2			50	89
Sm <sup>3+</sup>	-0.7			8	15
Eu <sup>3+</sup>	4.0	711	1530	-47	-85
Gd <sup>3+</sup>	0.0	1020	1410		
Dy <sup>3+</sup>	-100		1340		
Ho <sup>3+</sup>	-39			460	820
Tm <sup>3+</sup>	53			-630	-1120
Yb <sup>3+</sup>	22			-260	-470

<sup>a</sup> See text. <sup>b</sup> These have been used to estimate the magnitude of the pseudocontact shift. <sup>c</sup> The predicted shift on substituting one paramagnetic ion into the local coordination sphere of an yttrium.

shown to be dominated by a Fermi contact mechanism<sup>11</sup> and were approximately (except that of Yb<sub>2</sub>Sn<sub>2</sub>O<sub>7</sub>)<sup>24b</sup> proportional to the relative values of  $\langle S_z \rangle$ . The values for  $a_n$  are, however, likely to be smaller for <sup>89</sup>Y than for <sup>119</sup>Sn due to the more ionic nature of Y<sup>3+</sup> compared with Sn<sup>4+</sup>. This is therefore consistent with the much smaller shifts observed in the <sup>89</sup>Y spectra. For a contact mechanism to dominate, however, would require, at least for the Pr<sup>3+</sup>, Nd<sup>3+</sup>, and Eu<sup>3+</sup> compounds, that  $a_n$  has an opposite sign at <sup>89</sup>Y than at <sup>119</sup>Sn, although both yttrium and tin atoms are separated by the same number of atoms from the paramagnetic ion.

Given the smaller shifts for <sup>89</sup>Y compared with <sup>119</sup>Sn, and noting that the pseudocontact shift will make a similar contribution to each one, the pseudocontact shift will be a relatively more important term for <sup>89</sup>Y. The pseudocontact shift for a lanthanide ion is given by<sup>27</sup>

$$\sigma_p = \frac{-g^2\beta^2J(J+1)(2J-1)(2J+3)F}{60(kT)^2r^{-3}} \quad (i)$$

where  $g$  is the Landé  $g$  factor,  $r$  the Ln-N distance (N is the resonating nucleus), and  $F$  the angular factor.  $F$ , for a system with axial symmetry at the lanthanide site, which is the case for a cubic pyrochlore where the lanthanide site symmetry is  $D_{3d}$ , can be written as

$$F = A_2^0\langle r^2 \rangle (3 \cos^2 \theta - 1) \langle J || \alpha || J \rangle \quad (ii)$$

where  $\theta$  is the angle between the principal magnetic axis of symmetry at the lanthanide site and the Ln-N internuclear vector,  $\langle J || \alpha || J \rangle$  a numerical coefficient, and  $A_2^0\langle r^2 \rangle$  is a crystal field parameter at the Ln site, which for the pyrochlore structure is positive in sign.<sup>28</sup>

The first column of Table II gives the relative values of  $J(J+1)(2J-1)(2J+3)\langle J || \alpha || J \rangle W$ , where  $W$  is an additional multiplication factor, which incorporates extra terms that should be added to eq ii to take into account the mixing in of higher states,<sup>27</sup> particularly important for the ions Sm<sup>3+</sup> and Eu<sup>3+</sup>. The angle  $\theta$  that is likely to be applicable to substitution of a paramagnetic ion into the local coordination sphere of an yttrium atom

in the pyrochlore structure is marked in Figure 5; its value can easily be calculated and equals  $\cos^{-1} (2/3)^{1/2} (35.3^\circ)$ . Hence  $(3 \cos^2 \theta - 1) = +1.0$ . Using the values from Table II and taking  $3 \cos^2 \theta - 1 = +1.0$  and  $A_2^0\langle r^2 \rangle$  as positive, the predicted direction of the pseudocontact shift can be seen to be in accord with the direction of the experimentally observed shifts. A pseudocontact mechanism predicts shifts for Pr<sup>3+</sup>, Nd<sup>3+</sup>, and Sm<sup>3+</sup>-doped pyrochlores to be in the same direction, consistent with the experimentally observed shifts in the <sup>89</sup>Y spectra but not with those in the <sup>119</sup>Sn NMR.

The titanium pyrochlores will have larger values for  $A_2^0\langle r^2 \rangle$  compared to those in the tin analogues, as a consequence of their smaller unit cells volumes and to a lesser extent their larger axial distortions at the yttrium site.<sup>29,30</sup> This is in agreement with the generally greater shifts observed in the titanates. An estimate of the absolute magnitude of the pseudocontact shift may be made using values of  $A_2^0\langle r^2 \rangle$  calculated from Mössbauer data, since the rare-earth titanium and tin pyrochlores Ln<sub>2</sub>M<sub>2</sub>O<sub>7</sub> (Ln = Eu, Gd, Dy) have been studied with the <sup>151</sup>Eu, <sup>153</sup>Eu, <sup>155</sup>Gd, <sup>156</sup>Gd and <sup>161</sup>Dy isotopes,<sup>31</sup> and the electric field gradients (EFGs) at the rare-earth sites have been measured in these particular compounds. The EFGs can then be used to calculate the value of the crystal field parameter,  $V_2^0$ ,<sup>21</sup> which is related to the crystal field parameter  $A_2^0\langle r^2 \rangle$  by the following expression:

$$V_2^0 = (1 - \sigma_2)A_2^0\langle r^2 \rangle$$

The values of  $\sigma_2$ , an experimentally fitted factor, have been estimated for the lanthanide ions Eu<sup>3+</sup>, Gd<sup>3+</sup>, and Dy<sup>3+</sup> to be 0.78, 0.81, and 0.78, respectively.<sup>28</sup> The values of  $A_2^0\langle r^2 \rangle$  calculated by using these values are presented in Table II. In order to estimate the theoretical magnitude of the pseudocontact shift, the average value of  $A_2^0\langle r^2 \rangle$  within the stannate and titanate series was used, i.e., 865.2 cm<sup>-1</sup> for the Y<sub>2-y</sub>Ln<sub>y</sub>Sn<sub>2</sub>O<sub>7</sub> and 1424 cm<sup>-1</sup> for the Y<sub>2-y</sub>Ln<sub>y</sub>Ti<sub>2</sub>O<sub>7</sub> solid solutions. The values for  $r$ , the Ln-N distance, employed are those in the end-member compounds Y<sub>2</sub>Sn<sub>2</sub>O<sub>7</sub> and Y<sub>2</sub>Ti<sub>2</sub>O<sub>7</sub>, and are 3.667 and 3.569 Å, respectively;<sup>19,20</sup> the values calculated are given in Table II.

It is impressive that the predicted values of pseudocontact shifts are of the same order of magnitude as the experimental shifts themselves, especially since the value of  $A_2^0\langle r^2 \rangle$  used in the calculations is likely to differ considerably from the real value of  $A_2^0\langle r^2 \rangle$  in the yttrium sites in doped Y<sub>2</sub>Ti<sub>2</sub>O<sub>7</sub> and Y<sub>2</sub>Sn<sub>2</sub>O<sub>7</sub>.

It is clear from these predicted shifts that the pseudocontact shift will be an important term for <sup>89</sup>Y, unlike <sup>119</sup>Sn, and cannot be neglected. There are, however, at least three major reasons for the differences between the experimentally observed shifts and the predicted "pseudocontact" values. Firstly, there will be a contact term that is difficult to estimate and has not been taken into account. Another important factor is that the values of  $A_2^0\langle r^2 \rangle$  will differ from the values used to calculate the theoretical shifts, and the assumption that  $A_2^0\langle r^2 \rangle$  is independent of the dopant ion (i.e., the oxygen coordination does not relax as a dopant ion is introduced) will certainly not be valid. The  $x$  parameter for the lanthanide pyrochlores increases (albeit rather erratically) as the lanthanide ionic radius decreases,<sup>18</sup> resulting in a less distorted oxygen coordination around the lanthanide. Thus, assuming that the pyrochlore structure relaxes on doping with different cations, a dopant Yb<sup>3+</sup> ion will have a smaller axial distortion than a Pr<sup>3+</sup> ion and therefore should have a smaller value for  $A_2^0\langle r^2 \rangle$ . Finally, the theory developed by Bleaney<sup>27</sup> will not hold completely in the systems studied here, where the condition implicit in its derivation,

(24) (a) Golding, R. M.; Halton, M. P. *Aust. J. Chem.* **1972**, *25*, 2577-2581. (b) The Fermi contact involves polarization of the 5f and 6s orbitals of the lanthanide<sup>25</sup> ions and back-donation of the ligand electron density; however, in compounds containing Yb<sup>3+</sup> (and to a lesser extent Tm<sup>3+</sup>) ions, there is evidence<sup>26</sup> that a covalent mechanism becomes more important, involving direct interaction with the lanthanide 4f orbitals. The discrepancy in the ytterbium result may be due to an increased contribution of the latter mechanism (C.P.G., C.M.D., and A.K.C., unpublished results).

(25) Watson, R. E.; Freeman, A. J. *Phys. Rev.* **1967**, *156*, 251.

(26) McGarvey, B. R. *J. Chem. Phys.* **1976**, *65*, 955-968.

(27) Bleaney, B. J. *Magn. Reson.* **1972**, *8*, 91.

(28) Chien, C. L.; Sleight, A. W. *Phys. Rev.* **1978**, *B18*, 2031-2038.

(29) Calage, Y.; Pannetier, J. *J. Phys. Chem.* **1977**, *38*, 711-718.

(30) Gale, J. D.; Grey, C. P.; Cheetham, A. K., unpublished results.

(31) Bauminger, E. R.; Diamant, A.; Felner, I.; Nowik, I.; Ofer, S. *Phys. Lett. A* **1974**, *50*, 321. Armon, H.; Bauminger, E. R.; Diamant, A.; Nowik, I.; Ofer, S. *Phys. Lett. A* **1973**, *44*, 279. Almog, A.; Bauminger, E. R.; Levy, A.; Nowik, I.; Ofer, S. *Solid State Commun.* **1973**, *12*, 693. Armon, H.; Bauminger, E. R.; Ofer, S. *Phys. Lett. B* **1973**, *43*, 380. Armon, H.; Bauminger, E. R.; Diamant, A.; Nowik, I.; Ofer, S. *Solid State Commun.* **1974**, *15*, 543. Bauminger, E. R.; Diamant, A.; Felner, I.; Nowik, I.; Mustachi, A.; Ofer, S. *J. Phys. (Paris) C* **1976**, *6*, 49. Goldanskii, V. I.; Markov, E. F. In *Chemical Applications of Mössbauer Spectroscopy*; Goldanskii, V. I., Herber, R. H., Eds.; Academic Press: New York, 1968; p 103.

i.e., that the splittings of the ground-state terms are much smaller than  $kT$ , is not fulfilled. This would explain why the comparison between the experimental and predicted values for the shifts agree somewhat more closely for the stannate rather than the titanate samples since the ground-state splittings are likely to be larger for the latter. The temperature dependence of the observed shifts are in accord with this last suggestion; Bleaney's equation for the pseudocontact shift predicts a  $T^{-2}$  dependence that is close to that observed in the sample  $Y_{1.7}Nd_{0.3}Sn_2O_7$ , while the temperature dependence of the two titanates deviate considerably from this expectation. A contact shift mechanism predicts a  $T^{-1}$  dependence.<sup>24</sup> However, the separation of the two shift mechanisms on the basis of their different temperature dependences has proved extremely difficult in solution NMR, since in practice the magnetic anisotropy and therefore the pseudocontact shift deviates considerably from a linear  $T^{-2}$  dependence.<sup>32</sup> A more detailed prediction of the shifts and temperature dependences should take into account the relative populations of the ground-state levels.

One of the reasons for the broadness of the resonances of the doped samples, in comparison to pure materials, and their slight asymmetry (more clearly visible in spectra with less line broadening applied) is probably the presence of other smaller resonances obscured underneath the main resonance, resulting from yttrium local environments where a Ln<sup>3+</sup> ion is substituted into a more distant coordination sphere. That little change in sideband intensity is observed on doping lanthanides into the local coordination sphere is consistent with calculations of the magnitude of the dipolar coupling between the electron and nuclear moments<sup>33</sup> and will be discussed elsewhere.

Finally, it is likely that additional resonances, other than peak A, are not visible in the spectrum of  $Y_{1.7}Sm_{0.3}Sn_2O_7$  because the shifts would be too small to be resolved. New resonances were not resolved in samples containing Ho<sup>3+</sup> and Tm<sup>3+</sup> where the magnitude of both the pseudocontact and contact shift are predicted to be large. It may be that any new resonances are too broad to be visible, as it is difficult, with simple one-pulse experiments, to observe very broad peaks since a long preacquisition delay was used to avoid problems resulting from ringing of the probe.

### Conclusions

This paper has shown that <sup>89</sup>Y spectra can be obtained from diamagnetic solids doped with paramagnetic lanthanide ions. The relaxation times of <sup>89</sup>Y allowed the use of short recycle delay times for compounds containing paramagnetic ions, enabling the spectra to be accumulated more rapidly than for diamagnetic compounds.

This result is particularly important for  $I = 1/2$  nuclei such as <sup>89</sup>Y where the very long relaxation times observed in diamagnetic compounds will restrict the use of <sup>89</sup>Y MAS NMR.

Furthermore, changes in the local environment as yttrium ions are replaced by paramagnetic ions can easily be detected, each substitution of a paramagnetic ion into the first coordination sphere of the <sup>89</sup>Y atom producing a large additive shift. Since the relaxation times of nuclei close to paramagnetic ions are greatly reduced, the detection of these nuclei, which were often present in concentrations of less than 0.5% in the solid, became possible. The differing local environments could not have been distinguished by such techniques as X-ray diffraction. In addition, the composition of the limiting solid solutions, which were estimated from peak intensities, would have been difficult to obtain with comparable precision with diffraction methods. In the cerium-doped samples, the substitution of Ce<sup>3+</sup> into the pyrochlore lattice was also confirmed.

The shifts in the <sup>89</sup>Y spectra caused by the paramagnetic ions appear to have large contributions from a dipolar mechanism and are close to those predicted by Bleaney's equation,<sup>27</sup> at least at room temperature. This is in contrast to the shifts observed in the <sup>119</sup>Sn NMR of the lanthanide stannates Ln<sub>2</sub>Sn<sub>2</sub>O<sub>7</sub>, but is chemically reasonable in view of the nature of the Y–O and Sn–O bonds. Had <sup>89</sup>Y spectra been obtained from samples containing Ho<sup>3+</sup>, this would, were a shift obtained in the direction opposite to that observed in the Eu<sup>3+</sup> and Yb<sup>3+</sup> samples, have given convincing proof of a dominant pseudocontact mechanism. Further work is, therefore, required to separate more clearly the contributions from the through-bond and through-space interactions, but if this is possible, the geometric dependence of the pseudocontact shift should be of substantial value in structural studies of these and related materials. Since rare-earth-doped yttrates have well-established uses, for example, in the laser and phosphor industries,<sup>34,35</sup> it is hoped this study may be the basis of a method for probing rare-earth distributions and environments in a wide range of important yttrium-containing compounds.

Registry No. Y<sub>2</sub>Sn<sub>2</sub>O<sub>7</sub>, 12340-25-9; Y<sub>2</sub>Ti<sub>2</sub>O<sub>7</sub>, 12037-02-4; Y<sub>1.7</sub>Nd<sub>0.3</sub>Sn<sub>2</sub>O<sub>7</sub>, 126501-45-9; Y<sub>1.7</sub>Eu<sub>0.3</sub>Sn<sub>2</sub>O<sub>7</sub>, 126501-44-8; Y<sub>1.7</sub>Cl<sub>0.3</sub>Sn<sub>2</sub>O<sub>7</sub>, 126501-43-7; Y<sub>1.7</sub>Pr<sub>0.3</sub>Sn<sub>2</sub>O<sub>7</sub>, 126501-42-6; Y<sub>1.7</sub>Sm<sub>0.3</sub>Sn<sub>2</sub>O<sub>7</sub>, 126501-41-5; Y<sub>1.7</sub>Ho<sub>0.3</sub>Sn<sub>2</sub>O<sub>7</sub>, 126501-40-4; Y<sub>1.7</sub>Tm<sub>0.3</sub>Sn<sub>2</sub>O<sub>7</sub>, 126501-39-1; Y<sub>1.7</sub>Yb<sub>0.3</sub>Sn<sub>2</sub>O<sub>7</sub>, 126501-38-0; Y<sub>1.9</sub>Pr<sub>0.1</sub>Ti<sub>2</sub>O<sub>7</sub>, 126501-37-9; Y<sub>1.9</sub>Yb<sub>0.1</sub>Ti<sub>2</sub>O<sub>7</sub>, 126501-35-7; Y<sub>1.9</sub>Eu<sub>0.1</sub>Ti<sub>2</sub>O<sub>7</sub>, 126501-34-6; Y<sub>1.9</sub>Sm<sub>0.1</sub>Ti<sub>2</sub>O<sub>7</sub>, 126501-33-5; Y<sub>1.9</sub>Ce<sub>0.1</sub>Ti<sub>2</sub>O<sub>7</sub>, 126501-32-4; Y<sub>1.7</sub>Nd<sub>0.3</sub>Ti<sub>2</sub>O<sub>7</sub>, 126501-36-8; Y<sub>2-γ</sub>Ho<sub>γ</sub>Ti<sub>2</sub>O<sub>7</sub> (γ = 0.01–0.2), 126644-48-2; Y<sub>2-γ</sub>Tm<sub>γ</sub>Ti<sub>2</sub>O<sub>7</sub> (γ = 0.01–0.2), 126644-49-3; Y, 7440-65-5.

(32) Horrocks, D. DeW., Jr. *J. Magn. Reson.* 1977, 26, 333–339.

(33) Grey, C. P.; Brough, A. R.; Dobson, C. M., unpublished results.

(34) Leone, S. R.; Moore, C. B. *Chemical and Biochemical Applications of Lasers*; Moore, C. B., Ed.; Academic: New York, 1974; pp 1–27.

(35) Blasse, G.; Brill, A. *Philips Tech. Rev.* 1970, 10, 304–332.